Polymer-Peptide Conjugates

DOI: 10.1002/anie.200805768

Biotransformation on Polymer–Peptide Conjugates: A Versatile Tool to Trigger Microstructure Formation**

*Hans Kühnle and Hans G. Börner**

Recent progress in exploiting peptides and proteins for materials science applications has paved the way to tailor-made polymer–peptide conjugates.[1] Such bioconjugates have enabled advances in controlling nano- and microstructures. The translation of the biomimetic concept of "structure-based functions" would allow complex functional systems to be realized.[2,3] Bioconjugates can possess enzymatic activity, directed conductivity, or provide active interfaces to biological systems.[3,4] They can control silicification and crystallization processes, can mimic transmembrane channel systems or interact with a pharmaceutically relevant entity for drug-delivery applications.[5]

While the generation of specific functions in bioconjugates has been the focus of recent work, the control and regulation of such functions is now important. This control was initially demonstrated on polymer–protein bioconjugates, in which protein–ligand recognition could be regulated by temperature.[6]

Lynn and co-workers exploited the aggregation behavior of the amyloid peptide Aβ1–42 to organize a poly(ethylene oxide)(PEO)–peptide conjugate into core–shell nanofibers.[7] However, the self-assembly process was kinetically controlled. This peptide-guided organization process could be developed further by introducing a capable switch concept.[8,9] For that, temporary structure defects have been introduced into the peptide to suppress the self-assembly behavior of a peptide aggregator domain in a bioconjugate. The native peptide, and with it the aggregation tendency of the bioconjugate, could be reestablished by a pH-triggered O→N acyl transfer rearrangement in the switch-ester defects. This approach allowed the self-assembly kinetics of bioconjugates to be regulated in water and some organic solvents, leading to assemblies with complex, hierarchical structures.[9,10]

Posttranslational modification principles have great potential to provide regulative mechanisms for bioconjugates.[11] Particularly promising are the rapid phosphorylation and dephosphorylation of serine, threonine, or tyrosine side chains, which are often essential steps in signal-transduction pathways in biological systems.[12] Model peptides have been described recently, which exploit enzymatic phosphorylation and/or dephosphorylation to control the formation of coiled–coil bundles or peptide nanotubes.[13,14]

Herein we introduce the BioSwitch concept in which the function of peptide segments in polymer–peptide conjugates is regulated by enzymatic dephosphorylation of phosphothreonine residues. As a substrate that can be specifically manipulated by phosphatases, a poly(ethylene oxide)-*block*-peptide copolymer (PEO–peptide conjugate **I**, Scheme 1) was synthesized. The bioconjugate has a peptide segment with a primary structure containing five repeats of alternating threonine and valine diads ($(TV)_5$). As a result of the high propensity of valine and threonine to form β-sheets, and the alternating hydrophilic–hydrophobic pattern in the peptide strand, the peptide has a strong tendency to adopt the β-sheet motif. Five successive repeats of the Thr-Val unit are required to form stable β-sheet aggregates in water.[15] On the C-terminal side, *para*-nitrophenylalanine was introduced as a spectroscopic marker, and elongation with methionine and glycine gives a flexible segment between the aggregator domain and the PEO block.

Although this sequence would certainly result in kinetically controlled assemblies in water,[9] the self-organization tendency was temporarily suppressed by introducing three phosphothreonine units into the $(TV)_5$ peptide aggregator domain. The PEO–peptide conjugate **I** was synthesized with an inverse conjugation strategy by using semi-automated solid-phase supported peptide synthesis (SPPS) on a PAP

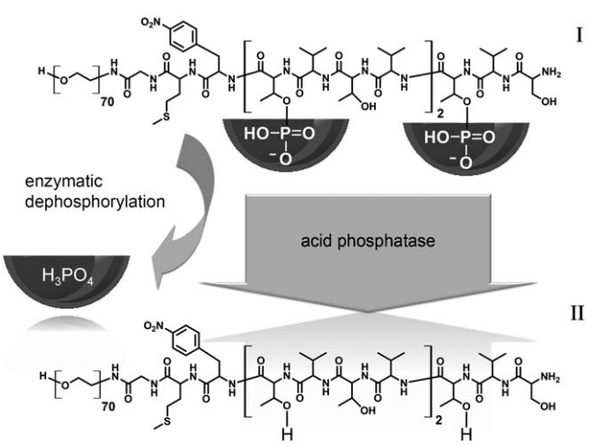

Scheme 1. The BioSwitch process (conditions: 0.1 mM trisodium citrate in Millipore water; pH 4.8–5.0 and ca. 0.5 units of an acid phosphatase).

[*] H. Kühnle, Dr. H. G. Börner
Max Planck Institute of Colloids and Interfaces
Research Campus Golm, 14424 Potsdam (Germany)
Fax: (+49) 331-567-9502
E-mail: hans.boerner@mpikg.mpg.de
Homepage: http://www.mpikg.mpg.de/kc/boerner/

[**] The work was supported by the Deutsche Forschungsgemeinschaft (Emmy Noether BO1762/2-3) and Max Planck Society. We thank M. Antonietti, A. Thomas, E. Krause, D. Gebauer, H. Stephanowitz, A. Heilig, R. Pitschke and A. E. F. Wächtler, M. Kühnle, and Erich C.

Supporting information for this article (descriptions of materials, instrumentations and methods, as well as experimental procedures) is available on the WWW under http://dx.doi.org/10.1002/anie.200805768.

resin (PEO attached polystyrene resin; see Supporting Information Scheme S1). The standard amino acid derivatives were coupled by automated Fmoc (9H-fluoren-9-ylmethoxy)-carbonyl) methods. *O*-phosphate modifications were selectively introduced into the side chains of Thr^{3}, Thr^{7}, and Thr^{11}, by the Fmoc-Thr(PO(OBzl)OH)-OH building block by applying bench-top methods. After sequential assembly of the peptide, the fully deprotected PEO–peptide conjugate **I** could be liberated from the support and the chemical structure was confirmed conclusively by means of NMR spectroscopy and MALDI-TOF mass spectrometry (Supporting Information).

The bioconjugate **I** was readily soluble in 0.1 mM citrate buffer (pH 5.0). Circular dichroism spectroscopy (CD) confirms that the phosphorylated peptide segments adopt a coil conformation with statistical chain-segment distribution (see Figure 2 and Supporting Information Figure S2) and this remains unchanged for at least 7 days. These results indicate that the β-sheet formation is effectively suppressed by the introduction of the three phosphothreonine units into the $(TV)_5$ aggregator domain. Moreover, the suppression of self-assembly by the $(TV)_5^{BioSwitch}$ was confirmed by atomic force microscopy (AFM) which shows no evidence of fibrillar structures, even after seven days (Supporting Information Figure S2).

To initiate the BioSwitch process, acid phosphatase was used as an enzyme to catalyze the hydrolysis of phosphate esters from the threonine side chains of **I**. The enzymatic dephosphorylation of the $(TV)_5^{BioSwitch}$ segment reconstitutes the native $(TV)_5$ segment of the bioconjugate (Scheme 1 and Figure 1, **I**→**II**). This change activates the aggregator domain and thus switches on the self-assembly process of the PEO–peptide conjugate. Acid phosphatase from potatoes is a commercially available orthophosphoric-monoester phosphohydrolase with a high substrate flexibility and an optimum activity in acidic environments (pH 4–5). The addition of the enzyme to I rapidly caused changes in the secondary structure of the peptide segment. Time-dependent CD spectroscopy shows a transition, shifting the structure of the peptide segment from statistical chain-segment conformation (random coil) to the β-sheet secondary structure (Figure 2).[13] Cotton effects, characteristic for β-sheets at $\lambda = 195$ nm (+) and 216 nm (−) developed gradually without

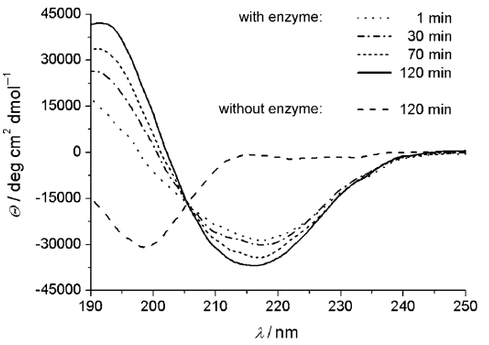

Figure 2. Dynamic CD spectroscopy showing the enzymatically triggered structure transition of the peptide segment from random coil to β-sheet (conditions: solution of **I** in 0.1 mM citrate buffer (c[**I**]$_0 = 0.33$ mg mL^{-1}); without enzyme and with enzyme, c[phosphatase]$_0 = 0.1$ mg mL^{-1} (0.5 U)).

inhibition phase and intensities reached a constant value within about 120 min. The occurrence of an isodichroic point in the CD spectra confirms a clean transition in secondary structure, involving a discreet shift between two distinct structure motifs. Thus CD suggests an effective BioSwitch process.

The biotransformation of the PEO–peptide conjugate can be investigated on the molecular level by ^{31}P NMR spectroscopy. The process of dephosphorylation was confirmed by the disappearance of the resonance characteristic for threonine *O*-phosphates accompanied by the appearance of a signal of free phosphoric acid (Supporting Information Figure S4). The amount of liberated phosphoric acid could be monitored by means of a colorimetric molybdate/malachite green phosphate assay (Supporting Information Figure S5). Figure 3 shows a rapid increase in concentration of phosphoric acid after addition of the phosphatase and suggests the end of the reaction after approximately 120 min. Dephosphorylation slows down at approximately 82% conversion, probably because of aggregation of the PEO–peptide conjugate that alters the accessibility of residual phosphate esters. These results indicate that despite the polymeric substrate, the enzymatic reaction on the bioconjugate occurs in a clean manner without an inhibition phase. Moreover, the dephos-

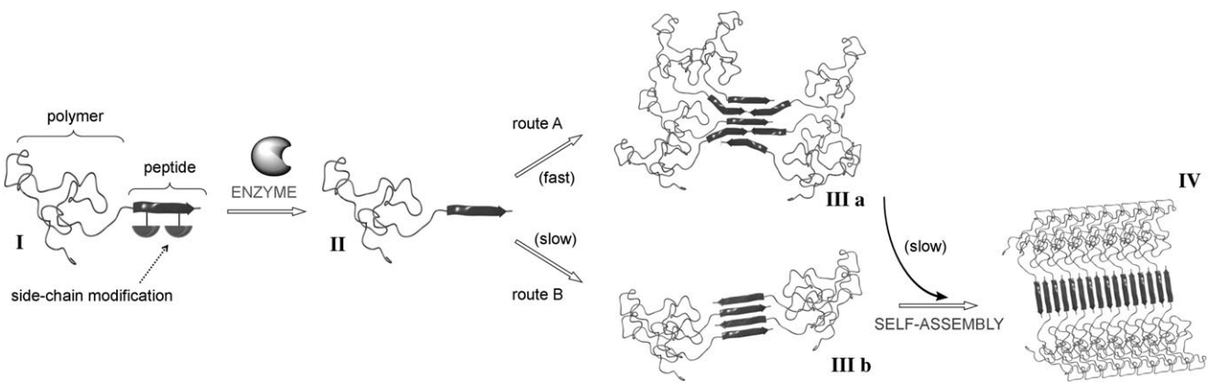

Figure 1. Schematic illustration of the BioSwitch process (**I**–**II**) and the suggested self-assembly mechanism of the activated bioconjugate (**III**–**IV**).

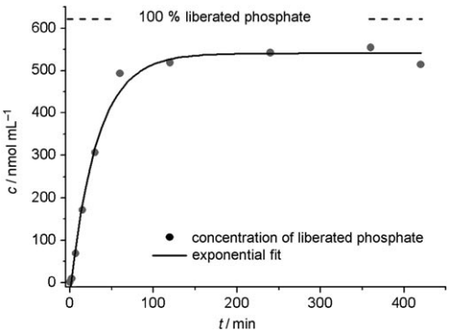

Figure 3. Colorimetric determination of the free phosphoric acid, as an indicator of the BioSwitch process for the enzymatic transformation of **I**→**II** ($c[\mathbf{I}]_0 = 1\ mg\,mL^{-1}$ in 0.1 mM citrate buffer (H_2O) and c[acid phosphatase]$_0 = 0.1\ mg\,mL^{-1}$ (0.5 U)).

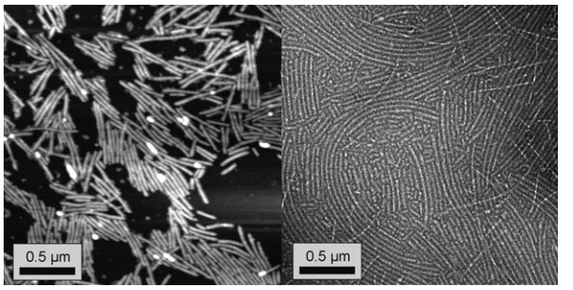

Figure 4. Microstructures formed by enzymatically triggered self-assembly of PEO–peptide conjugates. Structures visualized by AFM after 7 days (left, height image, $z = 10$ nm) and TEM micrograph of structures stained with uranyl acetate, after 10 days (right).

phorylation of **I** directly correlates with the structural coil to β-sheet transition of the peptide domain, because both processes proceed in approximately 2 h.

It is noteworthy, that despite the rapid biotransformation of the PEO–peptide conjugate and the practically simultaneous structural transition of the peptide, the self-assembly of the bioconjugates, although controlled, proceeds much more slowly. The first anisotropic objects with lengths of up to 100 nm could be observed by AFM after about one day. After about five days distinct fibrils with up to 300 nm in length were found. These fibers show further longitudinal growth up to about 2 µm over the following days (Figure 4 and Supporting Information Figure S11 B).

The resulting self-assembled fibrils were investigated in detail by analyzing microstructures obtained at least seven days after switching. This approach was required because the coexistence of unstructured material prevents the exact structural analysis at earlier stages of the self-assembly process. Figure 4 shows stiff and non-branched nanotapes with lengths up to 500 nm and rather uniform heights of approximately (2.9 ± 0.3) nm as determined by AFM (Supporting Information Figure S6). Transition electron microscopy (TEM) confirms the structures and suggests widths of about (16.9 ± 2) nm (Supporting Information Figure S8). The densely packed structures have two distinct features: 1) a high-contrast shell (that can be stained with uranyl acetate) of $2 \times (4.3 \pm 1)$ nm which can be attributed to the packed PEO chains and 2) a low-contrast core of (8.3 ± 1) nm that can not be stained by uranyl acetate (Figure 4, right). The core is consistent with previously described PEO–peptide β-sheet tapes, suggesting a rather hydrophobic peptide core.[16] The peptide organization motif could be directly correlated to the microscopic structures, using selected-area electron diffraction (TEM-SAED). The typical d spacing of 4.77 Å was observed, which is characteristic for the repeat distance of peptide β-strands adopting an extended β-sheet (Supporting Information Figure S7). This finding is supported by IR spectroscopy which show the typical amide I and amide II vibrational bands for a β-sheet structure (Supporting Information Figure S9).

Taking these observations into account, and considering the literature that describes the self-assembly of both β-sheet peptides and peptide–polymer conjugates,[2,16] a peptide-guided organization of the bioconjugate is suggested. The organization process is driven by the directed self-assembly of a peptide aggregator domain adopting a β-sheet motif and hence controlling the formation of fibrillar nanostructures. Previous investigations of related systems show that the widths of the primary nanotapes result from fully extended peptide β-strands, forming an anti-parallel β-sheet and forcing the PEO coils to pack laterally.[10,16,17] The height of the nanotapes of about 2.9 nm indicates that these core–shell nanotapes stack to form ribbons (double β-sheet tapes), as has been observed in analogous PEO–peptide conjugates.[9,16] Directional stacking of $(TV)_x$ β-sheets occurs as a result of the facial amphiphilicity of the β-sheets tapes, which have a hydrophobic valine face and a hydrophilic threonine face.

A careful investigation of the BioSwitch process was performed to elucidate the discrepancy between the rate of switching and the self-assembly. The enzyme concentration was systematically altered, by increasing the enzyme concentration from 0.03 to 0.1 to 0.3 $mg\,mL^{-1}$, while keeping the other parameters constant. As expected, CD spectroscopy indicates a clear correlation between enzyme concentration and the rate of the coil to β-sheet transition (Supporting Information Figure S10). With the lowest enzyme concentration the β-sheet formation required 320 min, the medium enzyme concentration it required 100 min, and with the highest enzyme concentration, only 30 min.

Although the fibrillogenesis proceeds much slower than the structural transition in the peptide segment, the enzyme concentration noticeably effects the self-assembly process. AFM measurements after 1, 5, and 10 days (Supporting Information Figure S11) revealed that the self-assembly proceeds similarly with the lowest and medium enzyme concentrations. Small amounts of fibrillar objects with lengths of up to about 100 nm can be found after 1 day. These small fibers coexist with large amounts of polydisperse globular structures, which are probably ill-defined aggregates of **II**. After 5 days, more of the extended structures are evident, and these show further longitudinal growth within the next days. The increase of the enzyme concentration to 0.3 $mg\,mL^{-1}$ accelerates the structural transition of the peptide segment to 30 min, however, even after 10 days only ill-defined materials could be found by AFM.

These results can be rationalized by comparing the BioSwitch triggered self-assembly process of PEO–peptide conjugates with the organization of misfolded proteins to amyloidal fibrils.[18] Figure 1 summarizes the proposed mechanism, which includes two possible assembly pathways that occur concurrently. The BioSwitch process transforms the PEO–peptide conjugate from the dormant state with suppressed aggregation tendency (**I**) into the active state that exhibits high aggregation tendency (**II**). These activated bioconjugates can either form ill-defined β-sheet assemblies (route A, **IIIa**) or follow route B to give defined β-sheet nanostructures (**IIIb**). While **IIIa** can be considered as a kinetically controlled metastable state, **IIIb** can be described as a thermodynamically controlled stable product.

The results suggest that under the applied conditions route A always dominates the early self-assembly process. However, at lower enzyme concentration, **II** is generated more slowly, allowing route B to occur as well. This results in the formation of a few, low-energy β-sheet nanostructures (**IIIb**). The presence of small amounts of such nuclei formed by route B can probably induce the fibrillogenesis (**IV**), making fiber growth under consumption of the ill-defined β-sheet structures possible. The mechanism is consistent with route A being exclusively favored at high enzyme concentration. Apparently, the fast formation of **II** suppresses route B and thus prevents the formation of nuclei, which ultimately suppresses the fibrillogenesis. Further kinetic studies combining time-dependent light scattering and analytical ultra centrifugation with seed experiments are required to evaluate the proposed mechanism. However, the intriguing analogies to biological amyloid fibrillogenesis are apparent, for which mechanisms are discussed involving "infectious" protein aggregates that can induce an autocatalytic protein β-sheet self-assembly.

In conclusion, a strategy has been demonstrated that utilizes enzymes to specifically manipulate peptide segments in peptide–polymer conjugates, enabling functions of bioconjugates to be regulated. A poly(ethylene oxide)–peptide conjugate including a $(TV)_5$-peptide aggregator domain was synthesized and the phosphorylation of the side chains of three threonine residues in the peptide sequence effectively prevents the self-assembly of the bioconjugate. Phosphatase was applied to catalyze the hydrolysis of the threonine-phosphate ester moieties which reinstalls the self-assembly tendency of the aggregator domain and triggers the peptide-guided organization of the bioconjugate to ultimately form fibrillar structures.

While the presented study shows the significance of phosphatases, molecular biochemistry provides a range of highly specific enzymes to switch, transform, modulate, or crosslink peptides. These enzymes are being further exploited in our work to switch properties of bioconjugates allowing the regulation of adsorption properties, binding capabilities, aggregation states, or bioactivity.

Received: November 27, 2008
Revised: May 7, 2009
Published online: July 8, 2009

Keywords: amyloid peptides · bioconjugates · enzymes · nanofibers · signal transduction

[1] a) J.-F. Lutz, H. G. Börner, *Prog. Polym. Sci.* **2008**, *33*, 1; b) H.-A. Klok, *J. Polym. Sci. Part A* **2005**, *43*, 1; c) J. C. M. van Hest, *Polym. Rev.* **2007**, *47*, 63.
[2] a) G. M. Whitesides, *Small* **2005**, *1*, 172; b) H. G. Börner, H. Schlaad, *Soft Matter* **2007**, *3*, 394; c) S. Förster, T. Plantenberg, *Angew. Chem.* **2002**, *114*, 712; *Angew. Chem. Int. Ed.* **2002**, *41*, 688; d) J. C. M. van Hest, D. A. Tirrell, *Chem. Commun.* **2001**, 1897.
[3] a) H. Frauenrath, E. Jahnke, *Chem. Eur. J.* **2008**, *14*, 2942; b) E.-K. Schillinger, E. Mena-Osteriz, J. Hentschel, H. G. Börner, P. Bäuerle, *Adv. Mater.* **2009**, *21*, 1562.
[4] a) H.-A. Klok, H. Schlaad *Adv Polym. Sci.* **2006**, *202*, 160; b) S. Tugulu, P. Silacci, N. Stergiopulos, H. A. Klok, *Biomaterials* **2007**, *28*, 2536; c) J. Hentschel, K. Bleek, O. Ernst, J.-F. Lutz, H. G. Börner, *Macromolecules* **2008**, *41*, 1073.
[5] a) S. Kessel, A. Thomas, H. G. Börner, *Angew. Chem.* **2007**, *119*, 9181; *Angew. Chem. Int. Ed.* **2007**, *46*, 9023; b) M. G. Page, N. Nassif, H. G. Börner, M. Antonietti, H. Cölfen, *Cryst. Growth Des.* **2008**, *8*, 1792; c) J. Couet, J. D. Jeyaprakash, S. Samuel, A. Kopyshev, S. Santer, M. Biesalski, *Angew. Chem.* **2005**, *117*, 3361; *Angew. Chem. Int. Ed.* **2005**, *44*, 3297; d) L. Hartmann, S. Häfele, R. Peschka-Süss, M. Antonietti, H. G. Börner, *Chem. Eur. J.* **2008**, *14*, 2025.
[6] P. S. Stayton, T. Shimoboji, C. Long, A. Chilkoti, G. H. Chen, J. M. Harris, A. S. Hoffman, *Nature* **1995**, *378*, 472.
[7] T. S. Burkoth, T. L. S. Benzinger, V. Urban, D. G. Lynn, S. C. Meredith, P. Thiyagarajan, *J. Am. Chem. Soc.* **1999**, *121*, 7429.
[8] a) M. Mutter, A. Chandravarkar, C. Boyat, J. Lopez, S. Dos Santos, B. Mandal, R. Mimna, K. Murat, L. Patiny, L. Saucede, G. Tuchscherer, *Angew. Chem.* **2004**, *116*, 4267; *Angew. Chem. Int. Ed.* **2004**, *43*, 4172; b) Y. Sohma, M. Sasaki, Y. Hayashi, T. Kimura, Y. Kiso, *Chem. Commun.* **2004**, 124.
[9] J. Hentschel, E. Krause, H. G. Börner, *J. Am. Chem. Soc.* **2006**, *128*, 7722.
[10] J. Hentschel, H. G. Börner, *J. Am. Chem. Soc.* **2006**, *128*, 14142.
[11] a) P. M. Gallop, M. A. Paz, *Physiol. Rev.* **1975**, *55*, 418; b) R. B. Rucker, C. McGee, *J. Nutr.* **1993**, *123*, 977; c) J.-H. Kim, S. Lee, K. Park, H. Y. Nam, S. Y. Jang, I. Y. K. Kim, H. Jeon, R.-W. Park, I.-S. Kim, K. Choi, I. C. Kwon, *Angew. Chem.* **2007**, *119*, 5881; *Angew. Chem. Int. Ed.* **2007**, *46*, 5779.
[12] a) A. C. A. Roque, C. R. Lowe, *Biotechnol. Bioeng.* **2005**, *91*, 546; b) M. Gallego, D. M. Virshup, *Curr. Opin. Cell Biol.* **2005**, *17*, 197.
[13] R. S. Signarvic, W. F. DeGrado, *J. Mol. Biol.* **2003**, *334*, 1.
[14] a) Z. M. Yang, G. L. Liang, L. Wang, X. Bing, *J. Am. Chem. Soc.* **2006**, *128*, 3038; b) R. J. Mart, R. D. Osborne, M. M. Stevens, R. V. Ulijn, *Soft Matter* **2006**, *2*, 822.
[15] K. Janek, J. Behlke, J. Zipper, H. Fabian, Y. Georgalis, M. Beyermann, M. Bienert, E. Krause, *Biochemistry* **1999**, *38*, 8246.
[16] a) D. Eckhardt, M. Groenewolt, E. Krause, H. G. Börner, *Chem. Commun.* **2005**, 2814; b) A. Agelli, I. A. Nyrkova, M. Bell, R. Harding, L. Carrick, T. C. B. McLeish, A. N. Semenov, N. Boden, *Proc. Natl. Acad. Sci. USA* **2001**, *98*, 11857.
[17] M. S. Lamm, K. Rajagopal, J. P. Schneider, D. J. Pochan, *J. Am. Chem. Soc.* **2005**, *127*, 16692.
[18] a) J. D. Harper, P. T. Lansbury, *Annu. Rev. Biochem.* **1997**, *66*, 385; b) F. E. Cohen, K. M. Pan, Z. Huang, M. Baldwin, R. J. Fletterick, S. B. Prusiner, *Science* **1994**, *264*, 530.

